



GEOSCIENCES

Role of the Southern Annular Mode in the sea level over the southern Blue Amazon

VENISSE SCHOSSLER, FRANCISCO E. AQUINO, JEFFERSON C. SIMÕES, RAFAEL C. SILVA, GABRIEL S. HOFMANN, DENILSON R. VIANNA, PEDRO H.R. LIRA, GIANLUCA POZZI & ANDRESSA M. DE OLIVEIRA

Abstract: Regional sea level rise varies from the global average and is influenced by climate variability. We studied sea level anomalies in southern Brazil from 1993 to 2022, finding increasing trend from 1993 to 2022. We used oceanic and atmospheric dynamics to understand the rapid sea level rise. Positive trends in the Southern Annular Mode and the South Atlantic Ocean subtropical gyre intensified wind stress curl and Ekman transport. If global warming continues and the Southern Annular Mode remains in a positive trend, sea level rise in southern Brazil is likely to persist and increase risks for the population in this low-lying coastal area.

Key words: South Atlantic Ocean, subtropical gyre, western boundary current, wind stress curl.

INTRODUCTION

An “exclusive economic zone” (EEZ) is an area of the ocean in which a coastal nation has jurisdiction over all resources. This zone extends 200 nautical miles (230 miles) beyond a nation’s territorial sea (NOAA 2024). In Brazil, around 95% of national oil is extracted in Brazilian jurisdictional waters, through which 95% of the country’s foreign trade also passes. This area, known as the “Blue Amazon,” has unique ecosystems and marine resources fundamental to regional economies. The Blue Amazon nomenclature was due to its similarity with the Amazon Forest (“Green Amazon”) in terms of dimensions, abundance of natural resources, and environmental, scientific, economic, and strategic importance. Through the Brazilian Continental Shelf Survey Plan (LEPLAC), Brazil requested international recognition from the United Nations for the expansion of Brazilian jurisdictional waters. Extending the Brazilian

continental shelf has continued for more than 70 years. It has allowed Brazil to expand its sovereignty, exceeding the limit of 200 miles, as established in the United Nations Convention on the Law of the Sea. In this long process, around 770 000 km², referring to the first submissions, and 170 000 km² of the current claims located to the South margin are already recognized (da Silva 2013), which belongs to the Brazilian southernmost states, that include Rio Grande do Sul (RS) (Figure 1).

The Rio Grande do Sul Coastal Plain extends for 605 km on the Brazilian southern coast (28°S–35°S, 48°W–54°W) with a population of 582 261 inhabitants (IBGE 2022). Its beaches are dissipative, characterized predominantly by the action of waves and coastal currents of the southeast quadrant, although the most recurrent are those of the northeast. The dominant wind of the region comes from the northeast (in the spring and summer months) and southwest

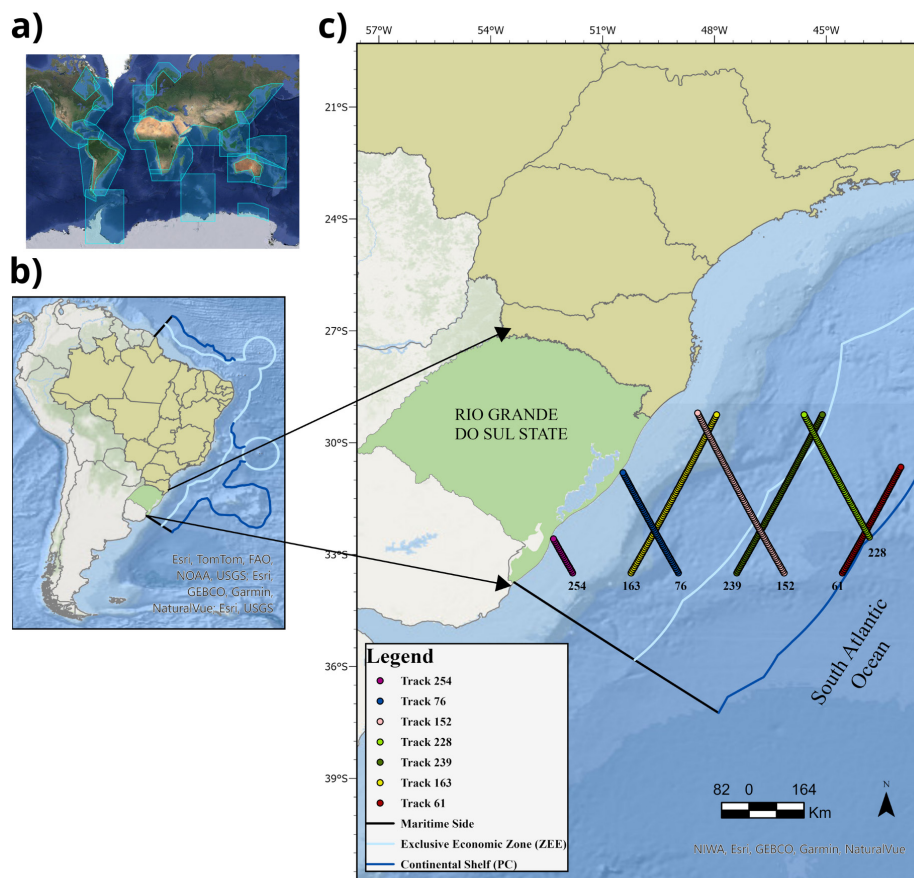


Figure 1. X-TRACK altimetry data and the localization of the study area are presented as follows: (a) The global coverage of X-TRACK, (b) the localization of the study area, and (c) the coast of the Rio Grande do Sul state in Brazil with the distribution of utilized tracks, and legal boundary of the exclusive economic zone and the continental shelf.

(in autumn and winter) (Almeida et al. 1997, 1999). The region has unique coastal vegetation and vast diversity in national environmental protection reserves. Schossler et al. (2018, 2020) presented results that prove the influence of SAM on extreme events in the study area. Global climate change poses a significant threat to low-lying coastal areas, making them particularly vulnerable to its effects.

Although sea level assessments on a global scale are critical to the future of humanity, evaluations from regional scales are essential when considering coastal security issues in specific locations. The regional scale includes local changes occurring in areas from tens to hundreds of kilometers. This scale may differ from the global average due to solid Earth processes or variations caused by ocean-atmosphere coupling (Stammer et al. 2013, Gregory et al.

2019, Hamlington et al. 2020a). In this way, atmospheric and oceanic circulation shifts can produce variations in regional sea levels as part of the dynamic process (Stammer et al. 2013, Han et al. 2019). Due to these variations, the studies that evaluate regional scales use the dynamic sea level (DSL) as an indicator to quantify changes since DSL is the sea surface high above the geoid, with the inverse barometer correction applied (Gregory et al. 2019). The DSL varies on interannual and decadal timescales, generating variability in sea level along the shore and between the coast and deep ocean, changing the trends (Boening et al. 2012, Han et al. 2019, Woodworth et al. 2019). Therefore, the coastal sea level reacts to remote or local changes in atmospheric and ocean circulations (Church et al. 2014, Kopp et al. 2015, Carson et al. 2016, Han et al. 2019). The long-term oscillations in the

climate system of the Earth, known as climate modes, represent another important source of variability for sea level on a regional scale.

Climate modes are a powerful part of climate variability spatial structure, with the amplitude represented for an index (Hernández et al. 2020). The climate modes affect coastal sea levels by forcing local winds and by remote influence from the ocean (Woodworth et al. 2019). Therefore, unlike long-term sea level changes, the decadal DSL changes are due to the natural climate modes and atmospheric-ocean coupling (Stammer et al. 2013). The leading mode of extratropical climate variability in the Southern Hemisphere is the Southern Annular Mode (SAM), defined by the pressure gradient between mid and high latitudes (Thompson & Solomon 2002, Fogt & Marshall 2020). SAM explains one-third of the variability in the extratropical atmospheric circulation in the Southern Hemisphere (Rogers & van Loon 1982, Kidson 1988, Kidson & Watterson 1999). The positive SAM phase is associated with intensification of the westerly winds over the circumpolar ocean ($\sim 60^\circ\text{S}$) and attenuation in subtropical latitudes. Zonally symmetrical SAM variations also affect the large-scale variability in oceans. They drive the Ekman transport to the north in all longitudes from the circumpolar region to around 30°S latitude (Thompson & Wallace 2000, Hall & Visbeck 2002). Additionally, the upwelling around Antarctica is higher due to mass continuity, leading to a sizeable vertical tilt of the isopycnals in the Southern Ocean and an increase in the Antarctic Circumpolar Current transport.

The trend towards positive SAM over the last 50 years is responsible for the high interannual variability of zonal and meridional wind tension, which intensifies ocean circulation in subtropical and subpolar oceans, thereby strengthening ocean gyres (Thompson & Solomon 2002, Willis et al. 2004, Roemmich et al. 2007). Alterations

in the atmospheric forcings, like wind stress and heat fluxes, lead to DSL changes (Lowe & Gregory 2006, Han et al. 2016, 2019). At the regional scale, the sea level changes may result from these variations in forcing factors, such as trends in wind stress (Cazenave & Moreira 2022). Wind stress is the horizontal force of the wind on the sea surface, and the wind stress curl (WSC) measures its rotation (Munk 1950). The WSC produces long westward-propagating Rossby waves, followed by sea level rise throughout the propagation track, and it is responsible for large-scale ocean circulation. Pronounced wind stress over ocean basins causes Ekman transport anomalies, increasing water accumulation in the southwest portion (Sverdrup 1947, Stommel 1948). This pumping causes a deepening of the tropical thermocline, raising the local sea level (downwelling) and leading to a shallower thermocline and a lower sea level in the east-sea portion (upwelling). Since the 1970s, wind stress has generated pronounced changes in the subtropical mid-latitude oceanic circulation (Cai et al. 2005). In this context, the notable changes in poleward migration of jet streams and west winds show that all extratropical circulation is moving in the poleward direction, including the subtropical edge of the Hadley cell (Fyfe et al. 1999, Thompson & Solomon 2000, Seidel & Randel 2007, Yang et al. 2020).

Many studies have shown that these shifts in atmospheric circulation are due to climate modes (Fyfe et al. 1999, Thompson et al. 2000). For example, in its positive phase, SAM favors the movement of the Hadley Cell poleward drive by troposphere temperature rise and tropopause height (Previdi & Liepert 2007, Monn & Ha 2019). The continued Hadley Cell southward expansion over the South Atlantic Ocean (SAO) takes changes to the South Atlantic Subtropical Anticyclone (SASA). SASA is the main feature of the atmospheric circulation over the SAO.

In this turn, when SAM is in a positive phase, SASA migrates poleward too (Sun et al. 2017, Reboita et al. 2019). Moreover, the extratropical atmospheric circulation changes are also associated with global warming, resulting in a poleward shift of ocean gyres and alterations in the marine heat transport, regional sea level, and coastal circulation (Yang et al. 2020). Over the past few decades, many research groups have focused on the effects of these changes on the different sea level patterns on regional scales worldwide (Sturges & Hong 1995, Hong et al. 2000, Han et al. 2010, Merrifield & Maltrud 2011, Yin & Goddard 2013).

Nevertheless, the consequences of changes in atmospheric circulation in the SAO for coastal regions of South America still need to be better understood. This necessity is particularly relevant due to the high susceptibility of the area to climatic modes, which profoundly influence its meteorological patterns (Silvestri & Vera 2003, Sen Gupta & England 2006, Schossler et al. 2018, 2020). Our objective is to evaluate the regional sea level variability on the Brazilian Southern territorial sea, called Blue Amazon (Figure 1). Therefore, we also assessed the possible relations between the regional sea level variations and changes in atmospheric circulation over the SAO that can affect this exclusive economic zone and, consequently, your population.

DATA AND METHODS

Sea level data

We used the software X-TRACK, designed by the *Laboratoire d'Etudes en Géophysique et Océanographie Spatiale* (LEGOS 2023) to overcome the related problems to satellite sea level altimetric measures in coastal areas (altimeter range, ionospheric, model dry and wet tropospheric, solid earth tide height, sea

state bias, geocentric ocean tide, geocentric pole ocean tide, dynamic atmospheric corrections). This software performs a post-processing algorithm that reexamines sea surface height altimetry data from the continental margin that processes the sea level anomalies (SLA) onto reference tracks with an approximately 6–7 km interval between each point (1 s). Regional SLA processing includes a low-pass filter with a 40 km cutoff frequency (see further details in Birol et al. 2017). The X-TRACK SLA values are obtained by Jason orbit: Topex-Poseidon, Jasons 1, 2, and 3. We used the 1993–2022 period from the X-TRACK Atlantic South America region (Figure 1) obtained from <https://www.aviso.altimetry.fr>. To get the annual SLA for the study area, we use 1073 cycles for each of the six tracks that cover it. By averaging the points and cycles, we could obtain the annual SLA to 1993–2022. We evaluate the serie trend using the straight-line equation, to determine the rate of increase or retreat, through the angular coefficient and its respective significance level (*p*-value). The adherence of the time serie to the trend line was also evaluated using the Pearson correlation coefficient.

For gridded sea level, we used the Global Ocean Gridded L4 Sea Surface Heights and Derived Variables (2023) by Copernicus, with a spatial resolution of 0.25° x 0.25°, period 1993–2022 (accessed at https://data.marine.copernicus.eu/viewer/expert?view=dataset&dataset=SEALEVEL_GLO_PHY_L4_MY_008_047).

Atmospheric and oceanic data

To evaluate changes in SASA and the winds, we generate mean sea level pressure (MSLP) and u/v winds components (10 m), vector, mean and anomalies fields from

ERA 5 (Copernicus 2023, Hersback et al. 2020) (<https://cds.climate.copernicus.eu/datasets>) To describe the interactions between variations in

atmospheric circulation and water transport, we use Ekman transport and WSC data from the U.S. Navy Fleet Numerical Meteorology and Oceanography Center – FNMOC (2023), with the following attributes 360 × 180 (geospatial distribution), from 6 h pressure (periodicity) (https://coastwatch.pfeg.noaa.gov/erddap/wms/erdlasFnWPr_LonPM180/index.html). To enhance the understanding of how SAM polarity influences the Southern circulation, we use the Marshall annual index (2003), which can be accessed from the following website: <https://climatedataguide.ucar.edu/climate-data/marshall-southern-annular-mode-sam-index-station-based>. Marshall uses SLP records from six stations (approximately at 65° S and 40° S). Finally, we analyzed the correlations between wind and MSLP and between SLA and WSC. Using Pearson's correlation, we compared all times for each grid point between the two variables.

Negative values indicate an inverse relationship between the variables and positive values indicate a direct relationship. The analyzed climatology is 1993–2022, and the climatology used for anomalies is 1960–1990.

RESULTS

The analysis reveals intriguing and significant connections between sea level fluctuations in the research area and the trend towards a positive Southern Annular Mode (SAM). We utilized six tracks covering the territorial sea of Rio Grande do Sul state to calculate sea level over a 30-year period (Figure 2a). All tracks exhibit similar patterns in the initial and final years of the time series (Figure 2b). However, there are variations in the sea level anomaly (SLA) values between 2007 and 2010. Notably, SLA values were predominantly below average from 1993 to 2001,

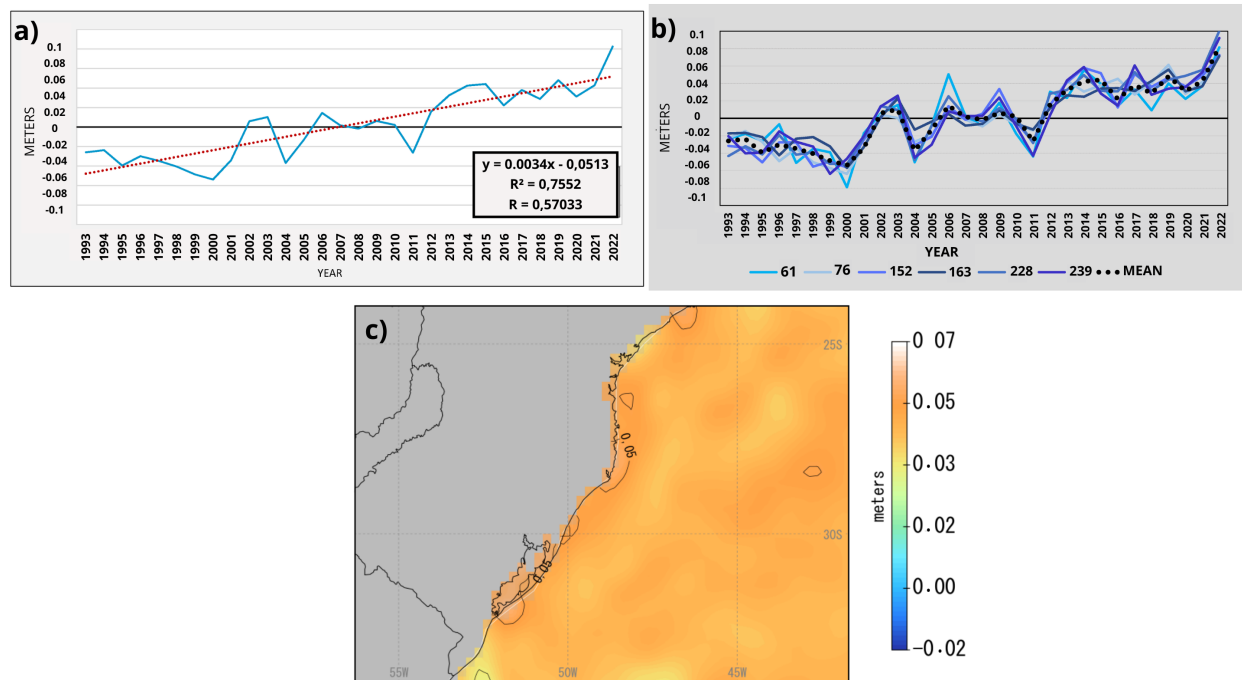


Figure 2. Sea level anomaly time series from 1993 to 2022. Figure (a) demonstrates a positive trend (p -value < 0.05) in the annual mean of X-TRACK sea level anomaly, (b) compares the annual values of the six X-TRACK tracks with their mean and, (c) the Copernicus sea level anomaly gridded data map. A solid black line in the map represents the significant values of sea level anomaly in meters. The yearly rate of change is 0.004 meters.

with an increase observed from 2001 to 2003, followed by subsequent fluctuations until 2008. After this period, there was a consistent rise in SLA, culminating in the highest point at the end of the 2009–2022 series, reflecting a positive trend ($R^2=0.7552$). To validate our findings, we cross-referenced the Copernicus SLA time series data (Figure 2c) and the map illustrates the Copernicus SLA climatology, revealing higher sea levels on the north coast compared to the extreme south of the state. Anomalies vary from -0.05 to $+0.08$ meters (0.004 m/year), with a confidence in the positive elevation trend ($p < 0.05$). We calculated the slope of the linear regression in variable units/time and estimated the error and significance of these trends ($r = 0.57$).

The MSLP data for the analyzed period shows a strengthening of the pressure gradient between medium and high latitudes (Figure 3). Analyzing these variations in MSLP and winds can provide insights into potential oceanographic variability, such as the development of the strength of Ekman transport due to the WSC. The figure 4 shows a slight expansion westward an poleward of the SASA compared to previous climatology (1960–1990). There is an increase in pressure gradient in South America direction, which indicates that the westward expansion of SASA and the positive SAM are contributing to this change (Figures 4a and b). Figures 3 and 4 show the average SAM index result (1.4) for the time series. The expansion of the Hadley cell is present, although discreet, becoming more evident when we observe the anomalies. We observed changes in the low-pressure belt around the Antarctica. On the outskirts of the Antarctica continent, the pressure is decreasing. We observe the strength of the Amundsen Sea Low and the SASA. Table I shows a positive correlation between the SAM index and the SLA across all six tracks. This positive correlation

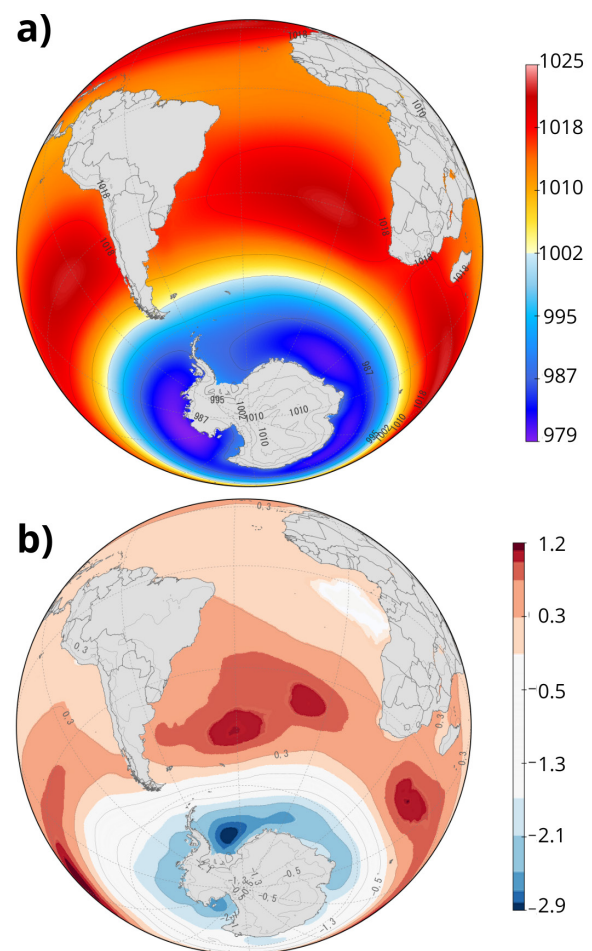


Figure 3. The mean sea level pressure (a) and the anomalies (b) in hectopascal for the 1993–2022 time series. The anomalies are referred to 1960–1990 climatology.

indicates that when the SAM is positive, the SLA is also positive.

The intensification of the pressure gradient between medium and high latitudes indicates varying atmospheric conditions, such as the westerlies around Antarctica patterns, related to climatology 1960–1990 (Figure 5). The composition of the zonal and meridional fields shows the strengthening of the westerlies in high latitudes, mainly between southern South America and the Antarctic Peninsula and the Indian and Southern Oceans (Figure 5a). The progressive strengthening of westerly winds in

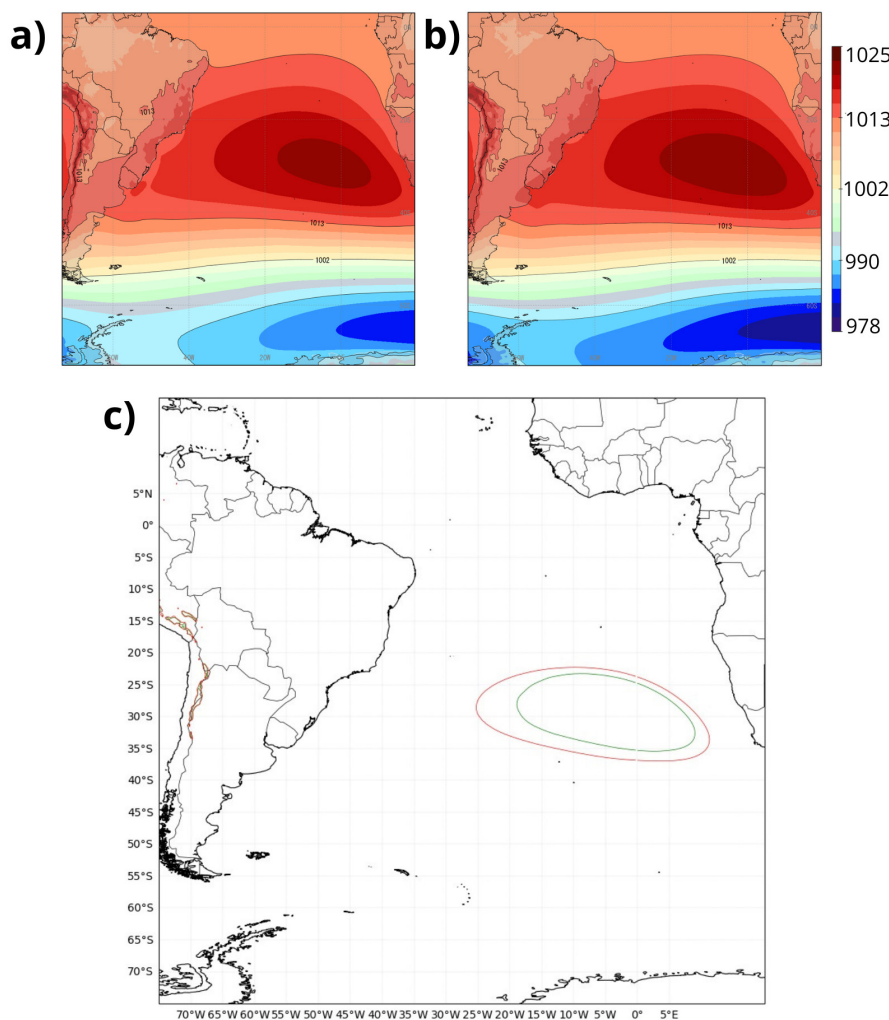


Figure 4. The mean sea level pressure between the South Atlantic and Southern Ocean in two different periods: (a) the 1960–1990 (1) and (b) 1993–2022 (2) climatology. Figure (c) compares the 1020 isobars of the South Atlantic Subtropical High in these two different periods: green (1) and red (2)—intervals of the three hectopascals.

high latitudes and easterly winds in medium latitudes is a typical characteristic of the positive SAM (Thompson & Solomon 2002). The westerlies flow across the plains of southern Patagonia, enhancing the Antarctic Circumpolar Current in your contact with SAO. The easterlies originated by SASA cross the Southern Brazil, Uruguayan, and Argentine coastal areas slowly. The increase in the pressure gradient between SASA and South America intensifies the winds on the southeast, northeast, and north Brazilian coasts. This pattern, added to the meridional flow increase toward the south over the west coast and north on the eastern coast of SAO, shows the strengthening of the SASA and the

Hadley cell poleward expansion. Noteworthy is the intensification of winds in the equatorial region of the SAO.

Figure 6 shows the spatial variability correlations between MSLP, zonal and meridional winds. A negative correlation between pressure and zonal wind (Figure 6a) can be seen, mainly in the center of the SASA and South American coast (around 15°S and 50°S). As zonal wind speeds increase, the mean sea level pressure decreases, and vice versa. In Figure 6b, we can see the correlation between the north-south component and MSLP. Our study is significant because it shows a positive correlation on the eastern boundary of the SAO. This process can

Table I. Correlation between SAM and sea level anomalies across the entire maritime zone and by each six tracks.

Tracks	Spearman Correlation	p-value
Rio Grande do Sul State continental shelf	0.095	0.618
RS61	0.045	0.815
RS76	0.121	0.524
RS152	0.113	0.553
RS163	0.215	0.254
RS228	0.1	0.6
RS239	0.12	0.528

lead to higher velocities in the SASA, resulting in the negative correlation with zonal winds shown in Figure 6a.

The WSC increased over the SAO in the studied period (Figure 7). The increase is a response to strengthening westerlies at high latitudes, i.e., the trend towards positive SAM. This trend also led to the intensification of easterly winds, which is associated with the expansion of the Hadley cell towards Antarctica. The WSC intensifies over the SAO longitudinally, with the highest values on the west coasts of Africa and South America. South of the Cape of Good Hope, we find another place with higher values. In the Brazil-Malvinas confluence, the area of positive WSC is a response to geostrophic flow due to the intensification of the westerlies in the Drake Passage. The greater WSC and Ekman transport in the Brazil-Malvinas confluence compels greater Ekman pumping, causing water transport to the north, the study area.

With the intensification of the westerlies and easterlies over the SAO and, consequently, the increase of the WSC, the Ekman transport grows towards the subtropical latitudes. The upwelling region, between 45°S and 60°S, supplies the downwelling at 30° S, especially in the study area where we can observe negative values, zero curl line, and low pumping. The

downwelling region on the Brazilian coast (around 20°S and 40°S) encompasses the location of the six SLA tracks used in this research (Figure 7b). The intensification of the WSC on the western coast of Africa contributes to the water transport to the coast of Brazil because it produces a more significant layer of upwelling. This strengthening is mainly due to increased meridional component from south to north. In this way, Figure 8 shows the correlation between SLA and WSC. It's possible to see that there are positive and negative correlations inside the black rectangle area, Blue Amazon of the Rio Grande do Sul state. It is also essential to highlight the growing downwelling and low Ekman pumping around the Antarctic continent (except in some coastal areas).

DISCUSSION AND CONCLUSIONS

Our study describes the role of the positive SAM in the sea level elevation on the Brazilian southern coast from 1993 to 2022. A recent study found an increasing sea level trend in the same region. It attributed it to the elevation of the steric height (halosteric and thermosteric) and changes in the oceanic mass (Ruiz-Estcheverry & Saraceno 2020). Here, we focused on analyses of the influence of the changes in southern

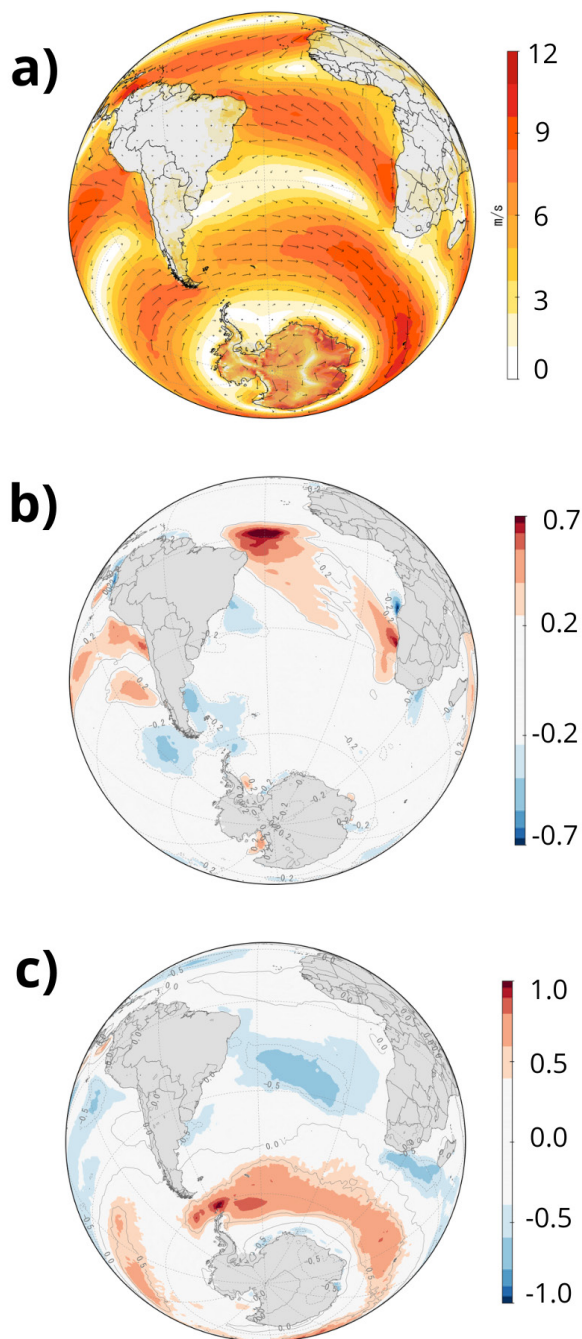


Figure 5. Wind fields for the period 1993–2022 (m/s-1). In (a) the composition of the u and v vectors, (b) and (c) the meridional and zonal wind anomalies, respectively. Anomalies calculated from the climatology 1960–1990.

atmospheric circulation, which SAM mainly controls.

The zonal component climatology over our study period indicates an intensification of the westerlies around Antarctica between 1993–2022 related to previous climatology, 1960–1990. The negative SLP anomalies detected over Antarctica are probably due to the strengthening of the polar vortex (Marshall 2003). Notoriously, the positive SAM produces stronger-than-average westerlies over the mid-high latitudes (50°S–70°S) and weaker westerlies in the mid-latitudes (30°S–50°S) (Thompson & Solomon 2002). The positive trend of the SAM creates a WSC maximum at 45°S and 60°S, and, consequently, Ekman transport northward (Hall & Visbeck 2002, Thompson & Solomon 2002). The meridional wind stress gradient controls changes in the WSC that characterize the amount of ocean water transported by the wind (Munk 1950). According to Cai et al. (2005), maximum wind stress in the Southern Hemisphere occurs at 60°S, generating maximum changes in WSC at 48° S. Our results show that the WSC maximum over the SAO extended southward, suggesting that it is a process associated with the migration of atmospheric and oceanic circulation poleward (Fyfe et al. 1999, Thompson & Solomon 2000, Cai et al. 2005, Seidel & Randel 2007, Yang et al. 2020). This process increases the sea surface height and alongshore currents over the Patagonian Continental Shelf and part of Brazil's southernmost coast (Bodnariuk et al. 2021).

Combes et al. (2023) established that internal ocean variability explains more than 50% of water transport on the southern Brazilian continental shelf through changes in Ekman transport associated with the strengthening of westerly winds. The study area receives transport offshore (~ 0.05 Sv at 35°S, ~ 0.1 Sv at 30°S), thereby resulting from tides and winds with significant contribution of the local wind forcing on the shelf circulation (NE and SW

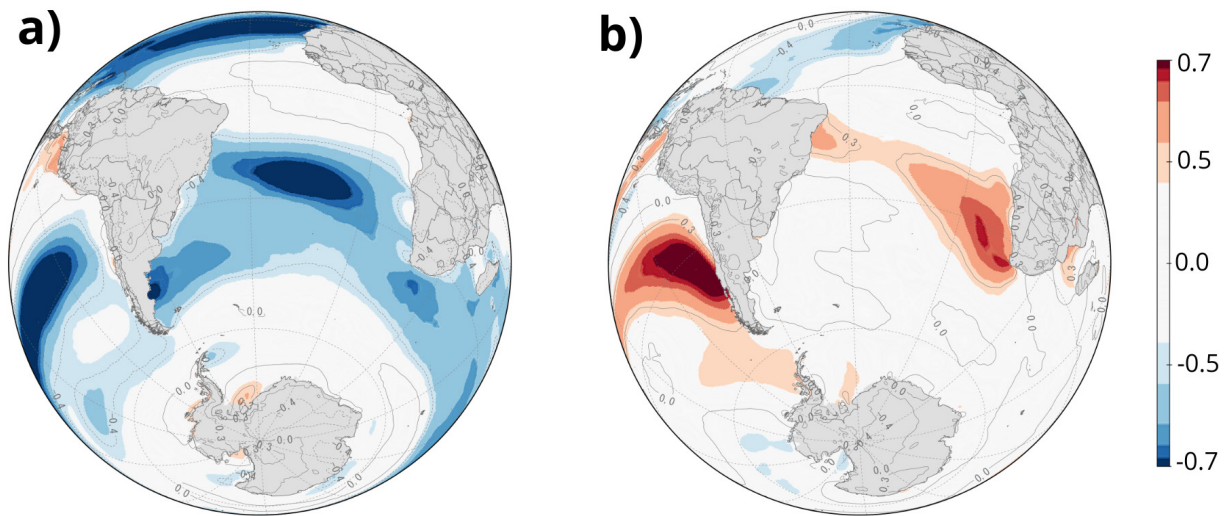


Figure 6. The maps illustrate the relationship between zonal (a) and meridional (b) winds and mean sea level pressure.

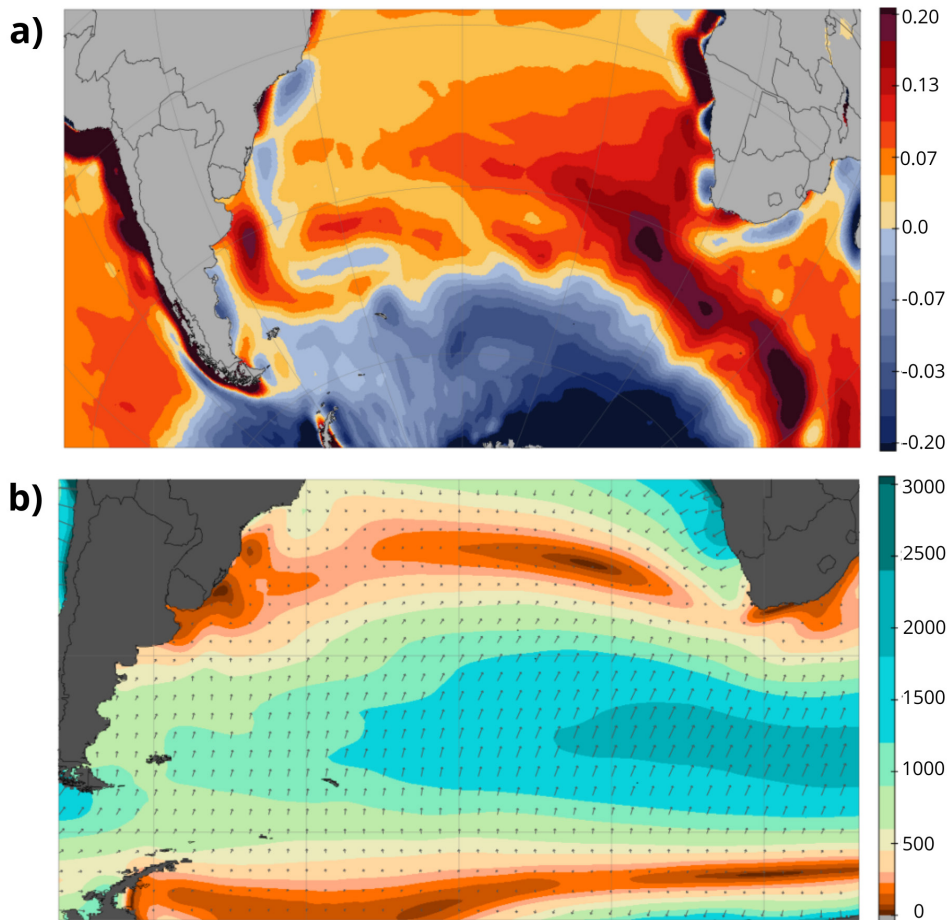


Figure 7. Regional view of the wind stress curl (MPa m^{-1}) and Ekman transport ($\text{Kg m}^{-1} \text{s}^{-1}$). In a) wind stress curl climatology and b) Ekman transport force (1993–2022).

predominantly), which complements the more significant forcing exerted by the Brazil Current (Combes et al. 2023). By the way, the Brazil-Malvinas Confluence is migrating southward together with the fronts and gyres related to the strengthened and southward displacement of the westerlies (Combes & Matano 2014, Leyba et al. 2019, Qu et al. 2019, Ruiz-Etcheverry & Saraceno 2020, Yang et al. 2020). Combes & Matano (2014) showed that, during 1993–2008, there was a generalized weakening of the Southern Ocean circulation associated with the weakening of the westerly winds that caused drift to the south of the Brazil-Malvinas Confluence. This migration enhanced the annual transport variability of the Malvinas Current at 40°S and WSC southward displacement. Our results for the same period also point to westerly negative anomalies and weaker WSC (not shown) related to the used time series (1993–2022). Other studies say that the variations in position of the Brazil-Malvinas Confluence are due to controlling factors, like WSC over the subtropical gyre and the Antarctic Circumpolar Current transport at the Drake

Passage (Matano 1993, Garzoli & Giulivi 1994, Wainer et al. 2000, Goni & Wainer 2001, Fetter & Matano 2008, Combes & Matano 2014).

The WSC variation caused by the positive SAM trend also provokes rotation of the mid-latitude oceanic circulation and the subtropical gyres poleward expansion. Past studies have identified that the most significant migration occurs on the western boundary of SAO, in the latitude band of 44°S and 54°S (Cai et al. 2005). During positive SAM, the westerlies get more robust due to a low-pressure system centered at 50°S that empowers the currents and the SASA, which results in easterly surface wind anomalies (Thompson & Wallace, 2000). This process strengthens the subtropical gyre and the Brazil Current (Schmid & Majumder 2018). Bodnariuk et al. (2021) find a high correlation between SAM positive and the alongshore wind anomalies over the Brazil and Malvinas currents (between 30°S and 55°S). They affirm that the alongshore wind anomalies induce stronger currents than usual due to sea surface height adjustment for offshore Ekman transport. Our results

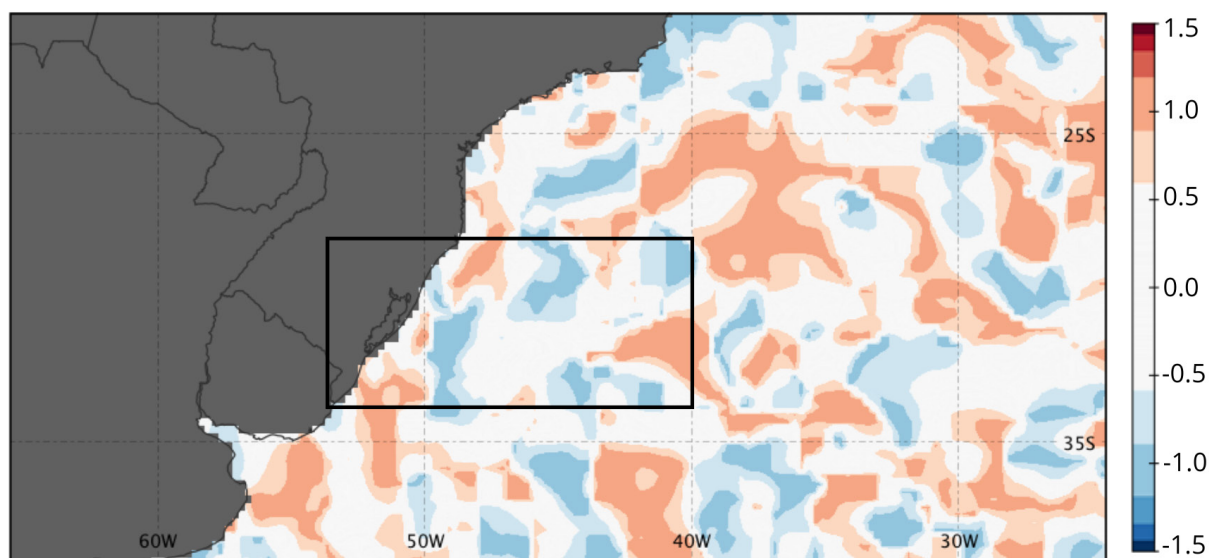


Figure 8. The Figure illustrates the correlation between sea level anomalies and wind stress curl within the study area, which is outlined by a black box (1993–2022).

showed that during the study period, the force exerted by WSC over SAO was predominantly positive, thereby increasing the downwelling area between 23°S and 35°S in the western boundary of SAO. We also recorded a vorticity intensification over the SAO and the expansion of the negative WSC in the study area, which, in turn, elevated the sea level. During the analyzed period, WSC intensified the downwelling on the Brazilian southern coast and upwelling on the African coast.

As part of global circulation, the large-scale change in the oceanic gyre has the potential to reshape the circulation of the ocean over the tropics, close to coastal regions, and also to change meridional overturning circulation (Lique & Thomas 2018, Yang et al. 2020). The strength of the trade winds imposes intensity on the South Atlantic subtropical gyre that experiences interannual to decadal variations associated with pressure variation in the SASA (Venegas et al. 1997, Sterl & Hazeleger 2003, Grodsky & Carton 2006). Shifting in gyres promotes a pronounced rise band at sea level over medium latitudes. This pattern overlaps with the global sea level average rise, thereby causing an extra threat to the islands and coastal regions at medium latitudes (Yin & Goddard, 2013). This mechanism is the same that can explain the observed sea level elevation in the study area once it is part of the South Atlantic subtropical gyre and is under the influence of SASA and SAM (Sun et al. 2017, Reboita et al. 2019). All these coupled ocean-atmosphere activities can vary with the polarity of the SAM (Thompson & Wallace 2000, Hall & Visbeck 2002, Thompson & Solomon 2002, Cai et al. 2005).

During 1993–2022 variations in pressure fields and winds occurred between high and medium latitudes due to the positive SAM trend. These processes increased Ekman transport to the study area region by WSC intensification,

which may result in a rising sea level. Internal variability of regional sea level is one of the contributing factors to its increase. However, recent studies have shown that anthropogenic forcing is an accelerating factor (Hamlington et al. 2020b). Climate models that use increased greenhouse gas effects as a variable suggest that the change observed in oceanic gyres results from global warming, as the displacement of atmospheric circulation leads to changes in gyres and subtropical fronts (Yang et al. 2020). The rise in global temperature causes changes in the coupling between atmospheric and oceanic circulations. Therefore, our results add to the understanding of the consequences of greenhouse gas increases in the atmosphere because they are associated with the positive trend of the SAM and suggest effects on regional temperature and sea level in the middle latitudes of the SAO. The risk to which the population of the south coast of Brazil is exposed justifies the monitoring of the causes and effects of global warming in the oceanic and atmospheric circulations of the SAO. The anthropogenic effects will be a superposition on the climate variability modes and natural static sea level patterns, forcing regionally the whole system. Furthermore, our results indicate the need to understand how changes in the austral atmospheric circulation may also be modifying the DSL of the rest of the Brazilian coast.

Acknowledgments

We thank the Conselho Nacional de Desenvolvimento Científico e Tecnológico (CNPq) - Project 465680/2014-3 (INCT da Criosfera), Project 151723/2022-2 (Postdoc project) and the Fundação de Amparo a Pesquisa do Estado do Rio Grande do Sul (FAPERGS) - Project 17/25510000518-0 for financial support. The altimetry data used in this study were developed, validated, and distributed by CTOH/LEGOS, France.

REFERENCES

- ALMEIDA LESB, ROSAURO NML & TOLDO JR EE. 1997. Análise Preliminar das Marés na Barra do Rio Tramandaí, RS. In: Simpósio Brasileiro de Recursos Hídricos, 12, Vitória. ABRH 1: 560-566.
- ALMEIDA LESB, ROSAURO NML, TOLDO JR EE & GRUBER NLS. 1999. Avaliação da Profundidade de Fechamento para o Litoral Norte do Rio Grande do Sul. In: Simpósio Brasileiro de Recursos Hídricos, 13, Belo Horizonte. ABRH CD-ROM: 8.
- BIROL F ET AL. 2017. Coastal applications from nadir altimetry: example of the X-TRACK regional products. *Adv Space Res* 59(4): 936-953. <https://doi.org/10.1016/j.asr.2016.11.005>.
- BODNARIUK N, SIMIONATO CG & SARACENO M. 2021. SAM-driven variability of the southwestern Atlantic shelf sea circulation. *Cont Shelf Res* 212: 104313. <https://doi.org/10.1016/j.csr.2020.104313>.
- BOENING C ET AL. 2012. The 2011 La Niña: So strong, the oceans fell. *Geophys Res Lett* 39(19). <https://doi.org/10.1029/2012GL053055>.
- CAI W, SHI G, COWAN T, BI D & RIBBE J. 2005. The response of the Southern Annular Mode, the East Australian Current, and the Southern mid-latitude ocean circulation to global warming. *Geophys Res Lett* 32: L23706. <https://doi.org/10.1029/2005GL024701>.
- CARSON M ET AL. 2016. Coastal Sea level changes observed and projected during the 20th and 21st century. *Clim Change* 134: 269-281. <https://doi.org/10.1007/s10584-015-1520-1521>.
- CAZENAVE A & MOREIRA L. 2022. Contemporary sea level changes from global to local scales: a review. *Proc R Soc A* 478: 20220049. <http://doi.org/10.1098/rspa.2022.0049>.
- CHURCH JA ET AL. 2014. Sea level change. *Climate change 2013: The physical science basis*, p. 1137-1216.
- COMBES V & MATANO RP. 2014. Trends in the Brazil/Malvinas Confluence region. *Geophys Res Lett* 41: 8971-8977. <http://doi.org/10.1002/2014GL062523>.
- COMBES V, MATANO RP & PALMA ED. 2023. Circulation and cross-shelf exchanges in the northern shelf of the southwestern Atlantic: Dynamics. *J Geophys Res Oceans* 128: e2023JC019887. <https://doi.org/10.1029/2023JC019887>.
- COPERNICUS: ERA 5 DATA. 2023. Copernicus Climate Change Service (C3S) Climate Data Store (CDS), <https://doi.org/10.24381/cds.6860a573>. Accessed 10 November 2023.
- DA SILVA AP. 2013. The new Brazilian claim on the sea: the extended continental shelf and the “Blue Amazon” Project. *Rev Bras Pol Int* 56(1): 104-120. <https://doi.org/10.1590/S0034-73292013000100006>.
- FETTER AFH & MATANO RP. 2008. On the origins of the variability of the Malvinas Current in a global, eddy permitting numerical simulation. *J Geophys Res Oceans* 113: C11018. <http://doi.org/10.1029/2008JC004875>.
- FNMOC – FLEET NUMERICAL METEOROLOGY AND OCEANOGRAPHY CENTER. 2023. FNMOC Wind and Ekman Transport Data, 360x180, Monthly, from 6-hr Pressure, <https://coastwatch.pfeg.noaa.gov/erddap/griddap/index.html?page=1&itemsPerPage=1000>. Accessed 30 October 2023.
- FOGT RL & MARSHALL GJ. 2020. The Southern Annular Mode: Variability, trends, and climate impacts across the Southern Hemisphere. *WIREs Clim Change* 11(4): e652. <https://doi.org/10.1002/wcc.652>.
- FYFE JC, BOER GJ & FLATO GM. 1999. The Arctic and Antarctic oscillations and their projected changes under global warming. *Geophys Res Lett* 26(11): 1601-1604. <https://doi.org/10.1029/1999GL900317>.
- GARZOLI SL & GIULIVI C. 1994. What forces the variability of the southwestern Atlantic boundary currents. *Deep Sea Res* 41(10): 1527-1550. [https://doi.org/10.1016/0967-0637\(94\)90059-0](https://doi.org/10.1016/0967-0637(94)90059-0).
- GLOBAL OCEAN GRIDDED L4 SEA SURFACE HEIGHTS AND DERIVED VARIABLES. 2023. Copernicus Marine Service Information (CMEMS). Marine Data Store (MDS). <https://doi.org/10.48670/moi-00148>. Accessed 20 November 2023.
- GONI G & WAINER I. 2001. Investigation of the Brazil Current front variability from altimeter data. *J Geophys Res* 106(C12): 31117-31128. <https://doi.org/10.1029/2000JC000396>.
- GREGORY JM ET AL. 2019. Concepts and Terminology for Sea Level: Mean, Variability and Change, Both Local and Global. *Surv Geophys* 40: 1251-1289. <https://doi.org/10.1007/s10712-019-09525-z>.
- GRODSKY SA & CARTON JA. 2006. Interannual variation of sea level in the South Atlantic based on satellite altimetry. *Proceedings of the Symposium on 15 Years of Progress in Radar Altimetry*, by Danesny, D. Noordwijk, Netherlands: European Space Agency, id.34. European Space Agency (Special Publication), p. 3.
- HALL A & VISBECK M. 2002. Synchronous Variability in the Southern Hemisphere Atmosphere, Sea Ice, and Ocean Resulting from the Annular Mode. *J Clim* 15(21): 3043-3057. [https://doi.org/10.1175/1520-0442\(2002\)015%3C3043:SVITSH%3E2.0.CO;2](https://doi.org/10.1175/1520-0442(2002)015%3C3043:SVITSH%3E2.0.CO;2).

- HAMLINGTON BD ET AL. 2020a. Investigating the acceleration of regional sea level rise during the satellite altimeter era. *Geophys Res Lett* 47(5): e2019GL086528. <https://doi.org/10.1029/2019GL086528>.
- HAMLINGTON BD ET AL. 2020b. Understanding of contemporary regional sea-level change and the implications for the future. *Rev Geophys* 58(3): e2019RG000672. <https://doi.org/10.1029/2019RG000672>.
- HAN W ET AL. 2010. Patterns of Indian Ocean sea-level change in a warming climate. *Nat Geosc* (3): 546-550. <https://doi.org/10.1038/ngeo901>.
- HAN W ET AL. 2016. Spatial Patterns of Sea Level Variability Associated with Natural Internal Climate Modes. *Surv Geophys* 38: 217-250. <https://doi.org/10.1007/s10712-016-9386-y>.
- HAN W ET AL. 2019. Impacts of Basin-Scale Climate Modes on Coastal Sea Level: a Review. *Surv Geophys* 40: 1493-1541. <https://doi.org/10.1007/s10712-019-09562-8>.
- HERNÁNDEZ A ET AL. 2020. Modes of climate variability: Synthesis and review of proxy-based reconstructions through the Holocene. *Earth Sci Rev* 209: 103286. <https://doi.org/10.1016/j.earscirev.2020.103286>.
- HERSBACH H ET AL. 2020. The ERA5 Global reanalysis. *Q J Meteorol Soc* 146(730): 1999-2049. <https://doi.org/10.1002/qj.3803>.
- HONG BG, STURGES W & CLARKE AJ. 2000. Sea Level on the U.S. East Coast: Decadal Variability Caused by Open Ocean Wind-Curl Forcing. *J Phys Oceanogr* 30(8): 2088-2098. [https://doi.org/10.1175/15200485\(2000\)030%3C2088:SLOTUS%3E2.0.CO;2](https://doi.org/10.1175/15200485(2000)030%3C2088:SLOTUS%3E2.0.CO;2).
- KIDSON JW. 1988. Indices of the Southern Hemisphere zonal wind. *J Clim* 1(2):183-194. [https://doi.org/10.1175/1520-0442\(1988\)001%3C0183:IOTSHZ%3E2.0.CO;2](https://doi.org/10.1175/1520-0442(1988)001%3C0183:IOTSHZ%3E2.0.CO;2).
- KIDSON JW & WATTERSON IG. 1999. The structure and predictability of the “high-latitude mode” in the CSIRO9 general circulation model. *J Atmos Sci* 56(22): 3859-3873. [https://doi.org/10.1175/15200469\(1999\)056%3C3859:TSA POT%3E2.0.CO;2](https://doi.org/10.1175/15200469(1999)056%3C3859:TSA POT%3E2.0.CO;2).
- KOPP RE, HAY CC, LITTLE CM & MITROVICA JX. 2015. Geographic Variability of Sea-Level Change. *Curr Clim Change Rep* 1: 192-204. <https://doi.org/10.1007/s40641-015-0015-5>.
- LEGOS. 2023. X-TRACK, Along track Sea Level Anomalies. http://doi.org/10.6096/CTOH_X-TRACK_2017_02. Accessed 12 October 2023.
- LEYBA IM, SOLMAN SA & SARACENO M. 2019. Trends in sea surface temperature and air-sea heat fluxes over the South Atlantic Ocean. *Clim Dyn* 53: 4141-4153. <https://doi.org/10.1007/s00382-019-04777-2>.
- LIQUE C & THOMAS MD. 2018. Latitudinal shift of the Atlantic Meridional Overturning Circulation source regions under a warming climate. *Nat Clim Chang* 8:1013-1020. <https://doi.org/10.1038/s41558-018-0316-5>.
- LOWE JA & GREGORY JM. 2006. Understanding projections of sea level rise in a Hadley Centre coupled climate model. *J Geophys Res Ocean* 111: C11014. <https://doi.org/10.1029/2005JC003421>.
- MARSHALL GJ. 2003. Trends in the Southern Annular Mode from Observations and Reanalyses. *J Clim* 16(24): 4134-4143. [https://doi.org/10.1175/1520-0442\(2003\)016%3C4134:TITSAM%3E2.0.CO;2](https://doi.org/10.1175/1520-0442(2003)016%3C4134:TITSAM%3E2.0.CO;2).
- MATANO R. 1993. On the separation of the Brazil Current from the coast. *J Phys Oceanogr* 23(1): 79-90. [https://doi.org/10.1175/1520-0485\(1993\)023%3C0079:OTSOTB%3E2.0.CO;2](https://doi.org/10.1175/1520-0485(1993)023%3C0079:OTSOTB%3E2.0.CO;2).
- MERRIFIELD MA & MALTRUD ME. 2011. Regional sea level trends due to a Pacific trade wind intensification. *Geophys Res Lett* 38(21): L21605. <http://doi.org/10.1029/2011GL049576>.
- MONN H & HA K. 2019. Distinguishing changes in the Hadley circulation edge. *Theor Appl Climatol* 139: 1007-1017. <https://doi.org/10.1007/s00704-019-03017-1>.
- MUNK WH. 1950. On the wind-driven ocean circulation. *J Atmos Sci* 7(2): 79-93. [https://doi.org/10.1175/1520-0469\(1950\)007%3C0079:OTWDOC%3E2.0.CO;2](https://doi.org/10.1175/1520-0469(1950)007%3C0079:OTWDOC%3E2.0.CO;2).
- NOAA - National Oceanic and Atmospheric Administration Ocean Exploration. 2024. What is the “EEZ”? <https://oceanexplorer.noaa.gov/facts/useez.html>. Accessed 30 March 2024.
- PREVIDI M & LIEPERT BG. 2007. Annular modes and Hadley cell expansion under global warming. *Geophys Res Lett* 34(22): L22701. <https://doi.org/10.1029/2007GL031243>.
- QU T, FUKUMORI I & FINE RA. 2019. Spin-up of the southern hemisphere super gyre. *J Geophys Res Oceans* 124(1): 154-170. <https://doi.org/10.1029/2018JC014391>.
- REBOITA MS, AMBRIZZI T, SILVA BA, PINHEIRO RF & ROCHA RP. 2019. The South Atlantic Subtropical Anticyclone: Present and Future Climate. *Front Earth Sci* 7(8): 15. <https://doi.org/10.3389/feart.2019.00008>.
- ROEMMICH D ET AL. 2007. Decadal spin up of the South Pacific subtropical gyre. *J Phys Oceanogr* 37(2): 162-173. <https://doi.org/10.1175/JPO3004>.
- ROGERS JC & VAN LOON H. 1982. Spatial Variability of Sea Level Pressure and 500 mb Height Anomalies over the

- Southern Hemisphere. *Mon Weather Rev* 110(10): 1375-1392. [https://doi.org/10.1175/1520-0493\(1982\)110%3C1375:SVOSLP%3E2.0.CO;2](https://doi.org/10.1175/1520-0493(1982)110%3C1375:SVOSLP%3E2.0.CO;2).
- RUIZ-ETCHEVERRY LA & SARACENO M. 2020. Sea Level Trend and Fronts in the South Atlantic Ocean. *Geosci* 10(218): 20. <https://doi.org/10.3390/geosciences10060218>.
- SCHMID C & MAJUMDER S. 2018. Transport variability of the Brazil Current from observations and a data assimilation model. *Ocean Sci* 14(3): 417-436. <https://doi.org/10.5194/os-14-417-2018>.
- SCHOSSLER V, AQUINO FE, REIS PA & SIMÕES JC. 2020. Antarctic atmospheric circulation anomalies and explosive cyclogenesis in the spring of 2016. *Theor Appl Climatol* 141: 537-549. <https://doi.org/10.1007/s00704-020-03200-9>.
- SCHOSSLER V, SIMÕES JC, AQUINO FE & VIANA DR. 2018. Precipitation anomalies in the Brazilian southern coast related to the SAM and ENSO climate variability modes. *Rev Bras de Recur Hidr* 23(14): 10. <https://doi.org/10.1590/2318-0331.231820170081>.
- SEIDEL DJ & RANDEL RJ. 2007. Recent widening of the tropical belt: Evidence from tropopause observations. *J Geophys Res* 112(D20): p 6. <https://doi.org/10.1029/2007JD008861>.
- SEN GUPTA A & ENGLAND MH. 2006. Coupled Ocean–Atmosphere–Ice Response to Variations in the Southern Annular Mode. *J Clim* 30 (21): 4457-4486. <https://doi.org/10.1175/JCLI3843.1>.
- SILVESTRI GE & VERA CS. 2003. Antarctic Oscillation signal on precipitation anomalies over southeastern South America. *Geophys Res Lett* 30(21): 2115. <https://doi.org/10.1029/2003GL018277>.
- STAMMER D ET AL. 2013. Causes for Contemporary Regional Sea Level Changes. *Annu Rev Mar Sci* 5: 21-46. <https://doi.org/10.1146/annurev-marine-121211-172406>.
- STERL A & HAZELEGER W. 2003. Coupled variability and air-sea interaction in the South Atlantic Ocean. *Clim Dyn* 21: 559-571. <https://doi.org/10.1007/s00382-003-0348-y>.
- STOMMEL H. 1948. The westward intensification of wind-driven ocean currents. *Transactions American Geophysical Union* 29(2): 202-206. <https://doi.org/10.1029/TR029i002p00202>.
- STURGES W & HONG BG. 1995. Wind Forcing of the Atlantic Thermocline along 32°N at Low Frequencies. *J Phys Oceanogr* 25(7): 1706-1715. [https://doi.org/10.1175/1520-0485\(1995\)025%3C1706:WFOTAT%3E2.0.CO;2](https://doi.org/10.1175/1520-0485(1995)025%3C1706:WFOTAT%3E2.0.CO;2).
- SUNX, COOK KH & VIZY EK. 2017. The South Atlantic subtropical high: climatology and interannual variability. *J Clim* 30(9): 3279-3296. <https://doi.org/10.1175/JCLI-D-16-0705.1>.
- SVERDRUP HU. 1947. Wind-Driven Currents in a Baroclinic Ocean; with Application to the Equatorial Currents of the Eastern Pacific. *Proc Natl Acad Sci USA* 33: 318-326. <https://doi.org/10.1073/pnas.33.11.318>.
- THOMPSON DWJ & SOLOMON S. 2002. Interpretation of recent Southern Hemisphere climate change. *Science* 296(5569): 895-899. <http://doi.org/10.1126/science.1069270>.
- THOMPSON DWJ & WALLACE JM. 2000. Annular modes in the extratropical circulation. Part I: Month-to-month variability. *J Clim* 13(5): 1000-1016 [https://doi.org/10.1175/15200442\(2000\)013%3C1000:AMITEC%3E2.0.CO;2](https://doi.org/10.1175/15200442(2000)013%3C1000:AMITEC%3E2.0.CO;2).
- VENEGAS SA, MYSAK LA & STRAUB DN. 1997. Evidence for interannual and interdecadal climate variability in the South Atlantic. *Geophys Res Lett* 23(19): 2673-2676. <https://doi.org/10.1029/96GL02373>.
- WAINER I, GENT P & GONI G. 2000. Annual cycle of the Brazil-Malvinas confluence region in the National Center for Atmospheric Research Climate System Model. *J Geophys Res* 105(C11): 26167-26177. <https://doi.org/10.1029/1999JC000134>.
- WILLIS JK, ROEMMICH D & CORNUELLE B. 2004. Interannual variability in upper ocean heat content, temperature, and thermosteric expansion on global scales. *J Geophys Res* 109(C12): 13. <http://doi.org/10.1029/2003JC002260>.
- WOODWORTH PL, MELET A & MARCOS M. 2019. Forcing Factors Affecting Sea Level Changes at the Coast. *Surv Geophys* 40: 1351-1397. <https://doi.org/10.1007/s10712-019-09531-1>.
- YANG H ET AL. 2020. Poleward shift of the major ocean gyres detected in a warming climate. *Geophys Res Lett* 47(5): 10. <https://doi.org/10.1029/2019GL085868>.
- YIN J & GODDARD PB. 2013. Oceanic control of sea level rise patterns along the East Coast of the United States. *Geophys Res Lett* 40(20): 5514-5520. <https://doi.org/10.1002/2013GL057992>.

How to cite

SCHOSSLER V, AQUINO FE, SIMÕES JC, SILVA RC, HOFMANN GS, VIANNA DR, LIRA PHR, POZZI G & DE OLIVEIRA AM. 2024. Role of the Southern Annular Mode in the sea level over the southern Blue Amazon. *An Acad Bras Cienc* 96: e20240592. DOI 10.1590/0001-376520240240592.

*Manuscript received on June 3, 2024;
accepted for publication on November 1, 2024*

VENISSE SCHOSSLER¹

<https://orcid.org/0000-0003-2825-9885>

FRANCISCO E. AQUINO¹<https://orcid.org/0000-0003-2993-1100>**JEFFERSON C. SIMÕES^{1,2}**<https://orcid.org/0000-0001-5555-3401>**RAFAEL C. SILVA¹**<https://orcid.org/0000-0001-6510-5290>**GABRIEL S. HOFMANN¹**<https://orcid.org/0000-0003-2525-8537>**DENILSON R. VIANNA¹**<https://orcid.org/0000-0002-4142-0189>**PEDRO H.R. LIRA¹**<https://orcid.org/0000-0002-6807-6226>**GIANLUCA POZZI¹**<http://orcid.org/0000-0002-1298-839X>**ANDRESSA M. DE OLIVEIRA¹**<https://orcid.org/0000-0003-2680-1757>

¹ Universidade Federal do Rio Grande do Sul,
Centro Polar e Climático, Av. Bento Gonçalves, 9090,
Agronomia, 91540-000 Porto Alegre RS, Brazil

² University of Maine, Climate Change Institute, Bryand Global
Sciences Building, 04469-5790 Orono, ME, United States

Correspondence to: **Venisse Schossler**

E-mail: venisse.schossler@ufrgs.br

Author contributions

VENISSE SCHOSSLER: material preparation, data collection and analysis, performed formal analysis, funding acquisition, investigation, methodology and wrote the first draft of the manuscript. RAFAEL C. SILVA, ANDRESSA M. DE OLIVEIRA and PEDRO H.R. LIRA: material preparation, data collection and analysis, methodology. JEFFERSON C. SIMÕES performed formal analysis, funding acquisition and supervision. FRANCISCO E. AQUINO: performed formal analysis, investigation and wrote the first draft of the manuscript. GIANLUCA POZZI: methodology. GABRIEL S. HOFMANN: wrote the first draft of the manuscript. All authors contributed to the study conception and design, commented on previous versions of the manuscript and read and approved the final manuscript.

